UC Berkeley
UC Berkeley Previously Published Works

Title

The hypothalamic–pituitary–gonadal axis controls muscle stem cell senescence through autophagosome clearance

Permalink

https://escholarship.org/uc/item/6r0867bx

Journal

Journal of Cachexia Sarcopenia and Muscle, 12(1)

ISSN

2190-5991

Authors

Kim, Ji-Hoon
Park, Inkuk
Shin, Hijai R
et al.

Publication Date

2021-02-01

DOI

10.1002/jcsm.12653

Peer reviewed

The hypothalamic–pituitary–gonadal axis controls muscle stem cell senescence through autophagosome clearance

Ji-Hoon Kim[1], Inkuk Park[1], Hijai R. Shin[2,3], Joonwoo Rhee[1], Ji-Yun Seo[1], Young-Woo Jo[1], Kyusang Yoo[1], Sang-Hyeon Hann[1], Jong-Seol Kang[1], Jieon Park[1], Ye Lynne Kim[1], Ju-Yeon Moon[4], Man Ho Choi[5] & Young-Yun Kong[1]*

[1]School of Biological Sciences, Seoul National University, Seoul, South Korea, [2]Department of Molecular and Cell Biology, University of California, Berkeley, CA, USA, [3]The Paul F. Glenn Center for Aging Research, University of California, Berkeley, CA, USA, [4]College of Pharmacy, The Catholic University of Korea, Gyeonggi-do, South Korea, [5]Molecular Recognition Research Center, KIST, Seoul, South Korea

Abstract

Background   With organismal aging, the hypothalamic–pituitary–gonadal (HPG) activity gradually decreases, resulting in the systemic functional declines of the target tissues including skeletal muscles. Although the HPG axis plays an important role in health span, how the HPG axis systemically prevents functional aging is largely unknown.
Methods   We generated muscle stem cell (MuSC)-specific androgen receptor (Ar) and oestrogen receptor 2 (Esr2) double knockout (dKO) mice and pharmacologically inhibited (Antide) the HPG axis to mimic decreased serum levels of sex steroid hormones in aged mice. After short-term and long-term sex hormone signalling ablation, the MuSCs were functionally analysed, and their aging phenotypes were compared with those of geriatric mice (30-month-old). To investigate pathways associated with sex hormone signalling disruption, RNA sequencing and bioinformatic analyses were performed.
Results   Disrupting the HPG axis results in impaired muscle regeneration [wild-type (WT) vs. dKO, $P < 0.0001$; Veh vs. Antide, $P = 0.004$]. The expression of DNA damage marker (in WT = 7.0 ± 1.6%, dKO = 32.5 ± 2.6%, $P < 0.01$; in Veh = 13.4 ± 4.5%, Antide = 29.7 ± 5.5%, $P = 0.028$) and senescence-associated β-galactosidase activity (in WT = 3.8 ± 1.2%, dKO = 10.3 ± 1.6%, $P < 0.01$; in Veh = 2.1 ± 0.4%, Antide = 9.6 ± 0.8%, $P = 0.005$), as well as the expression levels of senescence-associated genes, $p16^{Ink4a}$ and $p21^{Cip1}$, was significantly increased in the MuSCs, indicating that genetic and pharmacological inhibition of the HPG axis recapitulates the progressive aging process of MuSCs. Mechanistically, the ablation of sex hormone signalling reduced the expression of *transcription factor EB (Tfeb)* and Tfeb target gene in MuSCs, suggesting that sex hormones directly induce the expression of Tfeb, a master regulator of the autophagy–lysosome pathway, and consequently autophagosome clearance. Transduction of the Tfeb in naturally aged MuSCs increased muscle mass [control geriatric MuSC transplanted tibialis anterior (TA) muscle = 34.3 ± 2.9 mg, Tfeb-transducing geriatric MuSC transplanted TA muscle = 44.7 ± 6.7 mg, $P = 0.015$] and regenerating myofibre size [eMyHC⁺tdTomato⁺ myofibre cross-section area (CSA) in control vs. Tfeb, $P = 0.002$] after muscle injury.
Conclusions   Our data show that the HPG axis systemically controls autophagosome clearance in MuSCs through Tfeb and prevents MuSCs from senescence, suggesting that sustained HPG activity throughout life regulates autophagosome clearance to maintain the quiescence of MuSCs by preventing senescence until advanced age.

Keywords   Aging; Muscle stem cell; Muscle regeneration; Cellular senescence; Sex steroid hormones; Autophagy

Introduction

Adult muscle stem cells (MuSCs), also known as satellite cells, are maintained in a quiescent state within the skeletal muscle. Upon muscle injury, quiescent MuSCs become activated and enter myogenic commitment to repair damaged myofibres while maintaining the stem cell population through self-renewal.[1,2] In contrast, aged skeletal muscles fail to maintain stem cell quiescence, leading to a decline in MuSC number and functionality.[3–5] Previously, both environmental factors and intrinsic mechanisms in aged skeletal muscle have been proposed to affect the switch from quiescence to senescence.[6,7] Recent studies have shown that the entry into senescence and the premature differentiation of MuSCs in aged muscles result from the functional decline of autophagy and Notch signalling/calcitonin receptors, respectively.[8,9] However, the mechanism by which quiescent MuSCs maintain the physiological activities of autophagy and Notch signalling until the geriatric age is largely unknown.

The autophagy–lysosome pathway plays pivotal roles in protecting cells or organisms from stressful factors by avoiding waste accumulation.[10,11] Autophagy is a coupled process of self-degradation of cellular debris via autophagosome and autolysosome, which is composed of autophagosome formation, autophagosome fusion with the lysosome, and autophagosome clearance.[12] In the geriatric stage, both impaired basal autophagic flux and accumulated autophagosome in MuSCs lead to senescent and regenerative dysfunction of MuSCs.[9] Although a previous study reported that genetic mutants of Atg7, autophagy core gene, result in the entry of MuSCs into senescence, unlike geriatric MuSC, they already have defects in autophagosome formation.[9,13] Thus, the leading causes of age-associated autophagic decline and senescent MuSC are still elusive.

The hypothalamic–pituitary–gonadal (HPG) axis controls development, reproduction, and organismal aging. As puberty commences, hypothalamus secrets gonadotrophin-releasing hormone (GnRH) to stimulate luteinizing hormone and follicle-stimulating hormone in pituitary glands. These hormones travel in the blood stream to the ovary and testis to initiate the release of sex steroid hormones that circulate to the target tissues throughout life. Recent studies revealed that hypothalamic aging leads to systemic aging such as shortened life span, impaired memory, and muscle function, suggesting that the restoration of GnRH would be a potential strategy for combating aging-related health problems, through yet unspecified mechanisms of systemic action.[14,15] We previously reported that the physiological increase of sex hormones at puberty drives the conversion of MuSCs from proliferation to quiescence, which establishes a pool of adult MuSCs and re-establishes MuSCs after muscle regeneration upon injury.[16] Although several studies suggested that administration of androgens induces the proliferation of MuSCs in adults, most MuSCs remain quiescent despite high levels of sex steroid hormones after puberty (detailed in the review[17]). Thus, how high and declining levels of sex steroid hormones at adulthood and old age, respectively, play a role in MuSC physiology needs to be elucidated.

Here, using MuSC-specific androgen receptor (Ar) and oestrogen receptor 2 (Esr2) double knockout (dKO) mice and GnRH inhibition to mimic decreased serum levels of steroid hormones in aged mice, we clearly showed that the GnRH-sex steroid hormone axis prevents MuSCs from precocious senescence. As a mechanism, sex hormones directly regulate *transcription factor EB* (*Tfeb*) expression and thus mediate autophagosome clearance in MuSCs, suggesting that the HPG axis maintains MuSC stemness throughout lifetime.

Methods

Mice

All mouse lines were backcrossed onto a C57BL/6 background and were housed and handled according to the guidelines of the Institutional Animal Care and Use Committee at Seoul National University. C57BL/6J [wild-type (WT)] mice were used at designated ages, 4-month-old to 12-month-old, 20-month-old to 24-month-old, and 28-month-old to 30-month-old mice were used as young, old, and geriatric mice, respectively. To generate MuSC-specific Ar knockout mice, $Ar^{f/y}$ mice, inserted 2 loxP sites into exon 1,[18] were crossed with *Pax7-CreER* transgenic mice (stock. 017763, The Jackson Laboratory, Bar Harbor, ME, USA). *GFP-LC3* were kindly provided by Mizushima (Tokyo Medical and Dental University, Japan).[19] *Pax7-CreER*, *Rosa-diphtheria toxin A* (*DTA*) transgenic, and $Esr2^{-/-}$ knockout mice were purchased from The Jackson Laboratory. Tamoxifen (20 mg/mL in corn oil) (Sigma-Aldrich, St. Louis, MO, USA) was orally administered daily for five consecutive days (160 mg/kg body weight). Unless otherwise noted, male mice were used for all experiments.

Antide administration and dihydrotestosterone implantation

Three-month-old sex-matched and weight-matched littermate mice were subcutaneously (*s.c.*) injected with Nal-Lys gonadotropin releasing-hormone antagonist (Antide) (bioWorld, Dublin, OH, USA) at a dose of 6.0 mg/kg body weight weekly at the indicated times. Antide was dissolved in 20% propylene glycol and 0.9% saline. The duration of Antide treatment is determined according to experimental purposes. i.e. To investigate whether sex hormones directly regulate autophagy activity, we treated 3-month-old GFP-

LC3 transgenic mice for 4 months in which autophagic activity was altered to evaluate early events, while a pool of MuSCs were relatively maintained.

For sex hormone replenishment experiments, 5α-androstan-17β-ol-3-one C-IIIN [dihydrotestosterone (DHT), A8380; Sigma-Aldrich] was packed in 0.5-mm length silica tubes (Dow Corning, Midland, MI, USA). Silica tubes containing DHT were *s.c.* implanted. Implants were replaced every month to maintain serum DHT levels.

Muscle injury

For $BaCl_2$ injury, mice were anaesthetised with 2% avertin (0.02 mL/g body weight) and injected with 60 μL of $BaCl_2$ (1.2%; Sigma-Aldrich) in the tibialis anterior (TA) muscles. At the indicated times after injury, TA muscles were dissected, frozen in optimal cutting temperature compound (Sakura, Torrance, CA, USA) with liquid nitrogen, and stored at −80°C until analysis. Sections 7 μm thick were collected from TA muscles and stained with haematoxylin and eosin or Sirius Red or immunostained with indicated antibodies.

Muscle stem cell isolation by FACS

Muscle stem cell isolation was performed according to a previously reported protocol[20] with minor modifications (see Supporting Information, *Figure* S1). Limb muscles were mechanically dissected and dissociated in Dulbecco's modified Eagle's medium (DMEM) containing 10% horse serum (Hyclone, Logan, UT, USA), collagenase II (800 units/mL; Worthington, Lakewood, NJ, USA), and dispase (1.1 units/mL; StemCell Technologies, Vancouver, BC, Canada) at 37°C for 60 min. Digested suspensions were subsequently triturated and washed with DMEM to harvest mononuclear cells. Mononuclear cells were stained with Sca1-FITC (clone D7; BioLegend, San Diego, CA, USA), CD31-APC (clone MEC 13.3; BD Biosciences, Franklin Lakes, NJ, USA), CD45-APC (clone 30-F11; BD Biosciences), and Vcam1-Biotin (clone 429; BD Biosciences). Streptavidin-PE/Cy7 (BioLegend) was used as a secondary reagent. Stained cells were analysed and $Lin^-Vcam^+Sca1^-$ stem cells were isolated using a FACS Aria III cell sorter (BD Biosciences).

Lentivirus infection

Freshly isolated MuSCs plated in the RetroNectin coated plates and incubated for 16 h at 37°C in a cell culture incubator, and then, the lentiviral media were replaced. For *ex vivo* analysis, transduced MuSCs were incubated in cell culture incubator for the indicated time.

Cell culture and monitoring of autophagic flux

For MuSC cultures, isolated MuSCs were incubated at 37°C in DMEM containing 20% foetal bovine serum (HyClone) and basic fibroblast growth factor (2.5 nM/mL). HEK293T and C2C12 cells were cultured at 37°C in DMEM containing 10% foetal bovine serum. For the hormone inhibitor studies, C2C12 cells were incubated with DHT or 17β-oestradiol (E2, E8875; Sigma-Aldrich, 100 nM). Flutamide (Sigma-Aldrich), 1,3-bis(4-hydroxyphenyl)-4-methyl-5-[4-(2-piperidinylethoxy)phenol]-1H-pyrazole dihydrochloride (MPP; Tocris Bioscience, Bristol, UK), and 4-(2-phenyl-5,7-bis (trifluoromethyl)pyrazolo [1,5-a]pyrimidin-3-yl)phenol (PHTPP; Santa Cruz Biotechnology, Inc., Santa Cruz, CA, USA), selective antagonists of the androgen receptor (AR), oestrogen receptor alpha (ERα), and oestrogen receptor beta (ERβ), respectively, were used in indicated combinations and durations. All cell lines used in the study were cultured with antibiotics in a humidified incubator with 5% CO_2 and were regularly tested for mycoplasma contamination.

For measuring autophagic flux, freshly isolated quiescent MuSCs from muscles of vehicle-treated or Antide-treated GFP-LC3 mice were treated with bafilomycin A1 (10 nM; Sigma-Aldrich) 3 h before flow cytometry analysis. GFP-LC3 fluorescence signal was calculated by determining the FITC signal using FACS diva software (BD Biosciences).

To monitor autophagic flux by detecting endogenous LC3 proteins, freshly isolated MuSCs were treated with bafilomycin A1 (10 nM; Sigma-Aldrich) or vehicle (DMSO) 6 h before immunocytochemistry. Bafilomycin-treated MuSCs were attached on a slide glass by cytospin and were fixed by 4% paraformaldehyde in phosphate-buffered saline (PBS). The fixed MuSCs were washed with PBST (0.1% Tween20) several times and blocked at room temperature with blocking buffer (5% horse and goat serum in PBS) for 1 h and incubated with primary LC3 (1:200, MBL), p62 (1:200, sc-25575, Santa Cruz Biotech.) and polyubiquitinated conjugates ($Ub_{(n)}$, 1:100, FK1, Enzo) antibodies overnight at 4°C. The slides were washed with PBST several times and incubated with the appropriate secondary antibodies for 1 h at room temperature. The slides were counterstained with Hoechst (Invitrogen, Carlsbad, CA, USA) and mounted with Vectashield (H-1000; Vector Laboratories, Burlingame, CA, USA) after washing with PBST.

The mean fluorescence intensity of the area covered by LC3, p62, and Ub positive signalling was measured in microscopic images with Fiji software. Each dot is the averaged mean fluorescence intensity at least 50 cells from one mouse. Each fluorescence intensity value was normalized by the background value for the defined region of interest area.

To produce mCherry-GFP-LC3 lentivirus, HEK293T cells were transfected with the plasmid using Metafectene (Biontex, Munchen, Germany) according to the

manufacturer's protocol. The supernatant containing lentivirus was harvested 48 h after transfection and then used to infect MuSCs. Infected cells were treated with indicated sex hormone receptor antagonists for 12 or 24 h and fixed with 4% paraformaldehyde in PBS for 10 min; nuclei were stained with Hoechst (Invitrogen, Carlsbad, CA, USA). After washing, slides were mounted with Vectashield (Vector Laboratories, Burlingame, CA, USA). Because the low pH inside the lysosome quenches the fluorescent signal of GFP, with the mCherry-GFP-LC3 tandem construct, autophagosomes, and autolysosomes are displayed as yellow (GFP and mCherry) and red (mCherry) signals, respectively.

Statistical analysis

All statistical analyses were performed using GraphPad Prism 5 (GraphPadSoftware). Unless otherwise noted, all the error bars represent the SEM. Data were analysed using one-tailed *t*-test, Mann–Whitney U test (for a difference in mean), *F*-test (for variance test), analysis of variance (for comparison of significant difference in means among groups), Tukey's pairwise comparison test (after applying analysis of variance for multigroup comparison), Two-sample *t*-test was performed. The *P* value of <0.05 was considered statistically significant at the 95% confidence level. The additional descriptions of the methods are in the supporting information.

Results

Sex hormones prevent enhanced senescence of muscle stem cells

To investigate whether sex steroid hormones directly act on MuSCs, androgen and oestrogen receptors were genetically inactivated using $Pax7^{CreER};Ar^{f/y}$ ($Ar^{\Delta SC}$) and $Esr2^{-/-}$ mice, respectively,[21–23] and muscle regeneration assay was performed using $BaCl_2$-induced injury. Although both $Ar^{\Delta SC}$ and $Esr2^{-/-}$ mice showed normal muscle regeneration, $Ar^{\Delta SC};$ $Esr2^{-/-}$ dKO mice showed impaired muscle regeneration (*Figures* 1A and 1B, S2A, and S2B). Female dKO mice also exhibit decreased size of regenerating myofibres compared with WT mice, indicating that either Ar or Esr2 signalling is required for proper muscle regeneration regardless of sex differences (*Figure* S2C and S2D). To confirm cell-intrinsic regenerative failure by sex hormone signalling ablation, we performed *ex vivo* proliferation assays for freshly isolated WT or dKO MuSCs (*Figure* S1A–S1C). Ninety-six hours after incubation, the number of colony-forming (*Figure* S2E and S2F) and percentage of 5-ethynyl-2'-deoxyuridine (EdU) incorporating MuSCs (*Figure* S2E and S2G) were significantly reduced in dKO MuSCs compared with those in WT MuSCs. The

functional defects of dKO MuSCs were further confirmed by the decrease in proliferation (Ki67), myogenic activation (MyoD), and myogenic differentiation (Myogenin) expression 3 days after muscle injury (*Figure* 1C–1H). These data suggested that cell-intrinsic deletion of the sex hormone receptor leads to impaired MuSC function. Because the impairment of cell cycle re-entry and myogenic lineage progressions could result from cellular senescence,[9,24,25] we further examined senescence-associated phenotypes in freshly isolated MuSCs. The expression of DNA damage marker (γH2AX), senescence-associated β-galactosidase (SA-β-Gal) activity, and expression levels of senescence-associated genes, $p16^{Ink4a}$ and $p21^{Cip1}$,[26,27] were significantly increased in dKO MuSCs compared with those in controls (*Figure* 1I–1M). Taken together, these results show that sex hormones prevent enhanced senescence of MuSCs in a cell-intrinsic manner.

Sex hormones regulate autophagosome clearance

To gain insight into how disruption of sex hormones leads to the precocious senescence of MuSCs, we performed RNA sequencing of dKO MuSCs. Interestingly, in addition to steroid hormone-responsive genes, autophagy-related and lysosome genes were down-regulated in dKO MuSCs compared with those in WT MuSCs (*Figure* 2A–2C). LC3, p62, and polyubiquitinated proteins were accumulated in dKO MuSCs even without bafilomycin (Baf) treatment, whereas Atg5-12 complex, essential for autophagosome formation, did not show any differences. (*Figure* 2D–2H). We observed that autophagy flux was impaired in dKO MuSCs 1 month after sex hormone signalling disruption (*Figure* S3A–S3G), while the expressions of senescence markers, *p16* and *p21* (*Figure* S3H), and regenerative capacity of MuSCs were comparable with those of control (*Figure* S3I and S3J). Intriguingly, the amount of reactive oxygen species in MuSCs was gradually increased after the ablation of sex hormone signalling and then eventually reached the level similar to that of geriatric mice (*Figure* S3K), suggesting that prolonged impairment of autophagic flux by sex hormone reduction results in cellular senescence.

To investigate how sex hormones are implicated in autophagic flux, we further analysed the RNA sequencing data for autophagy-related and lysosome genes[28] using Ingenuity Pathway Analysis. Interestingly, the autophagy master regulator, Tfeb,[29] was the highest scored upstream regulator based on the changes in expression caused by the knockout of *Ar/Esr2* (*Figure* 2I and *Table* S1). The autophagy–lysosome pathway is tightly controlled and coordinated at the level of gene expression by *Tfeb*,[28–31] and Tfeb plays a central role in cellular and organismal aging through the autophagy–lysosome pathway.[32–34] Thus, these suggest that the sex hormone signalling might be implicated in the regulation of autophagy via Tfeb expression.
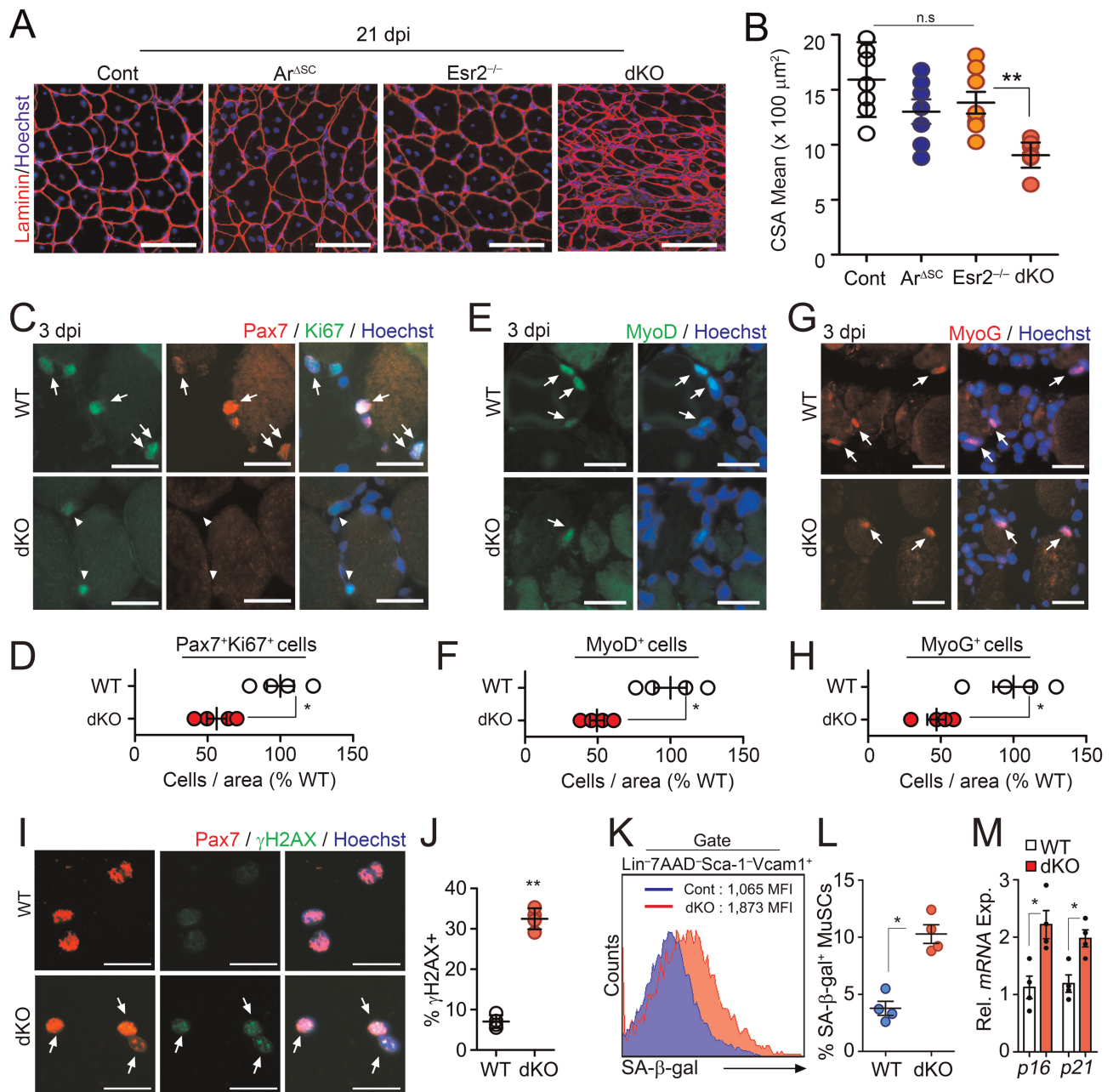
Figure 1 Accelerated aging phenotypes of muscle stem cells (MuSCs) in the absence of intrinsic sex steroid receptor signalling. (A–H) Three-month-old WT (Con), $Pax7^{CreER};Ar^{f/y}$ (Ar$^{\Delta SC}$), $Esr2^{-/-}$ and $Pax7^{CreER};Ar^{f/y};Esr2^{-/-}$ (dKO) mice were orally administered with tamoxifen (Tmx) for five consecutive days. Tibialis anterior (TA) muscles were injured by BaCl$_2$ injection at 6 months after Tmx administration. TA muscles were analysed at 21 days post-BaCl$_2$ injury (dpi). Immunohistochemical (IHC) staining for laminin (A) and quantification of mean cross-section-area (CSA) of regenerating TA muscles (B). Representative IHC images and quantification of Pax7 and Ki67 costaining (C and D) in TA muscles at 3 dpi. Arrows and arrowheads indicate Pax7$^+$Ki67$^+$ and Pax7$^+$Ki67$^-$ cells, respectively. Representative images and quantification of MyoD (E and F) and Myogenin (MyoG, G and H) staining in TA muscles at 3 dpi. Arrows indicate MyoD + or MyoG + cells. (I) Immunostaining and (J) quantification for Pax7 and γH2AX in freshly isolated MuSCs from uninjured mice. Arrows indicate Pax7$^+$γH2AX$^+$ cells. (K) Flow cytometry analysis of SA-β-Gal activity, and (L) quantification of SA-β-Gal$^+$ cells in isolated MuSCs. (M) Relative mRNA expression of senescence-associated genes in MuSCs. Scales: 100 (A), 50 (C, E, and G), and 20 μm (I). Comparisons by one-way ANOVA with Tukey's post hoc test (B), unpaired t-test (D, F, H, J, and M), and Mann–Whitney U test (L). Bars, mean ± SEM. A, B; n = 7 TA muscles from 4 animals per group and C–M; 4 animals per group *$P < 0.05$, **$P < 0.01$. The detailed procedure of CSA quantification applied throughout this study is described in the supporting information.
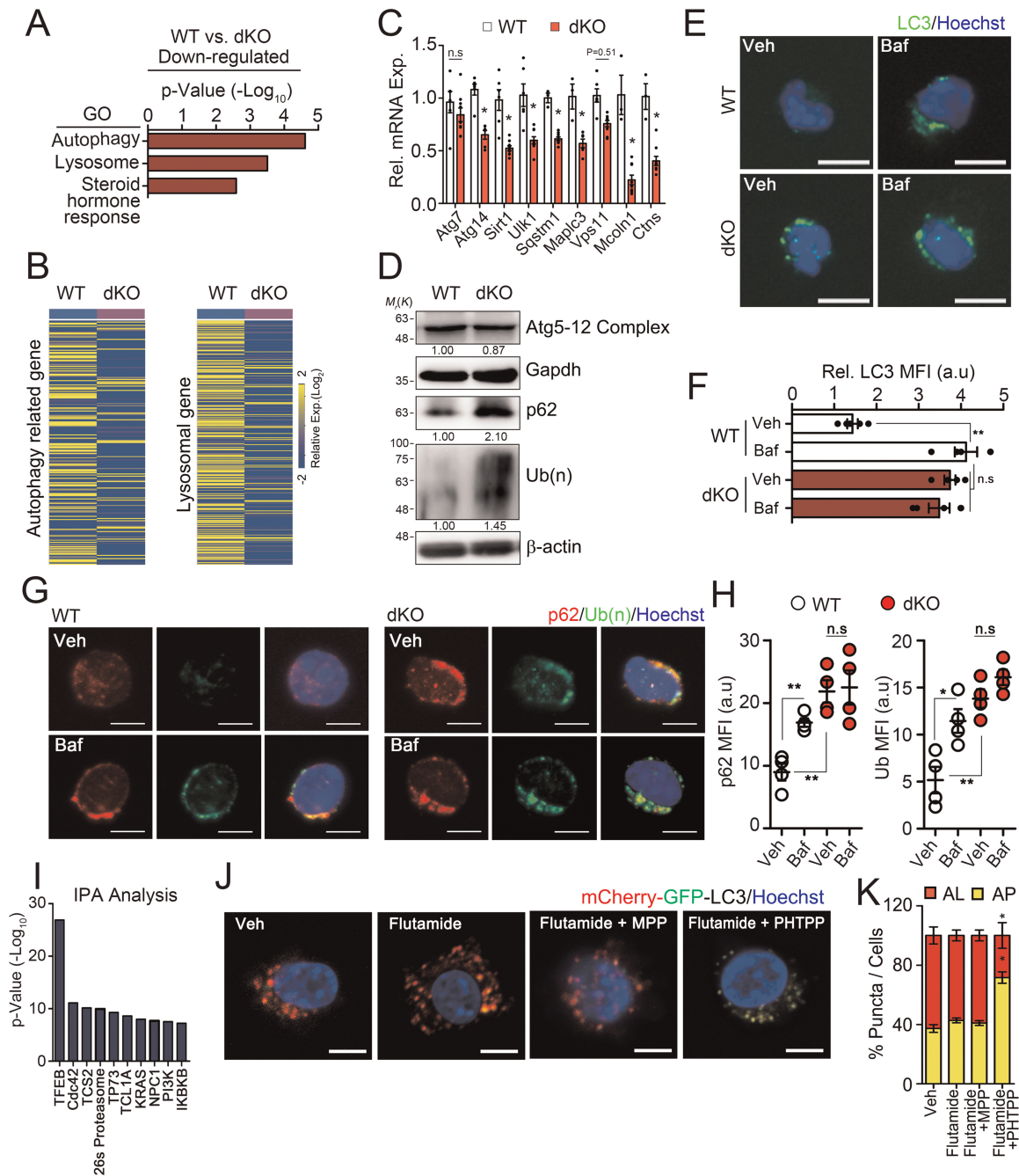
Figure 2 Regulation of autophagy–lysosome system in muscle stem cells (MuSCs) by sex steroid receptor signalling. (A–I) Three-month-old WT and dKO mice were orally administered with tamoxifen for 5 days, and then, MuSCs were isolated from hindlimb muscles 6 months after tamoxifen treatment. Freshly isolated MuSCs were analysed by RNA sequencing 2868 genes satisfying fc 2. Z-score were used for normalization. Gene ontology (GO) analysis (A). Heat map for relative expression of autophagy-related and lysosomal genes in WT and dKO MuSCs (B). Autophagy genes were obtained from the Human Autophagy Database (http://autophagy.lu) and the mouse Autophagy Database (http://www.tanpaku.org/autophagy). Lysosomal genes were obtained from Lysosomal gene database (http://lysosome.unipg.it). The confirmation of autophagy and lysosomal genes in MuSCs by qPCR analysis (C). Western-blot analysis of Atg5-12 complex, p62, polyubiquitinated proteins in isolated MuSCs. Relative band densities were indicated below each blot (D). Immunostaining (E and G) and quantified mean fluorescence intensity (MFI) for LC3 and p62/poly-ubiquitin (F and H) in MuSCs with (Veh) or without Bafilomycin (Baf), respectively. IPA analysis for bioinformatic prediction of putative upstream regulators of down-regulating autophagy and lysosomal genes in dKO MuSCs compared with WT MuSCs (I). (J) Representative images and (K) quantifications of GFP and mCherry fluorescent. MuSCs expressing mCherry-GFP-LC3 were treated with indicated inhibitors for 24 h. Flutamide, an Ar inhibitor; MPP, an Esr1 inhibitor; PHTPP, an Esr2 inhibitor; AL, autolysosome, AP; autophagosome. Comparisons by one-way ANOVA with Tukey's post hoc test (F, H, and K) and unpaired *t*-test (C). Scales, 10 μm, bars, mean ±SEM. *n* = 4 animals per group; *$P < 0.05$, **$P < 0.01$. The detailed procedure and sample size of MFI quantification applied throughout this study are described in Methods. dKO, double knockout; WT, wild-type.

To investigate whether sex hormones indeed regulate autophagic flux, the freshly isolated MuSCs from WT limb muscles were transduced with lentiviral mCherry-GFP-LC3 reporter for 24 h. Because GFP fluorescence is quenched by the acidity of the lysosome, GFP⁺mCherry⁺ (yellow) puncta indicate autophagosomes, whereas GFP⁻mCherry⁺ (red) puncta indicate autolysosomes.[29] mCherry-GFP-LC3–transduced MuSCs were further cultured in complete medium containing both DHT and E2 for 24 h with varying combinations of flutamide, an androgen-receptor DNA-binding antagonist[35]; MPP, an oestrogen receptor-1 antagonist[36]; or PHTPP, an oestrogen receptor-2 antagonist.[37] Although treatment with any single inhibitor did not affect the autophagic flux, the combined inhibition of Ar and Esr2 markedly blocked autophagosome clearance (*Figure* 2J and 2K), suggesting that the sex hormones might be implicated in MuSC senescence through the regulation of autophagosome clearance.

Sex hormones control autophagosome clearance in muscle stem cells through Tfeb transcriptional activation

To examine whether sex hormones induce autophagosome clearance by regulating *Tfeb* expression, we assessed the *Tfeb* expression level in C2C12 cells cultured under the various hormonal culture conditions. Importantly, *Tfeb* expression was markedly decreased by the combined inhibition of Ar and Esr2 (*Figure* 3A and 3B). To further confirm that sex hormones activate autophagosome clearance through Tfeb, we conducted a reporter assay using a luciferase construct containing four repeats of coordinated lysosomal expression and regulation (CLEAR) elements (4× CLEAR).[38] Consistently, luciferase activity was reduced by the combined inhibition of Ar and Esr2 (*Figure* 3C). To investigate how sex steroid hormones regulate *Tfeb* expression, we performed a chromatin-immunoprecipitation assay against Ar in MuSCs. Ar was recruited to androgen response elements in the *Tfeb* promoter in young MuSCs (*Figure* 3D and 3E). We confirmed that the expression levels of Tfeb target genes were up-regulated upon sex hormone treatment in a dose-dependent manner (*Figure* 3F). Together, these results show that sex hormones control autophagosome clearance in MuSCs through Tfeb transcriptional activation. Consistently, *Tfeb* and Tfeb target gene expression were decreased in MuSCs from dKO mice compared with those in controls (*Figure* 4E).

To further examine whether Tfeb expression can restore impaired autophagosome clearance in dKO MuSCs, we transduced them with lentiviral vectors containing control [Lv-Cont-IRES-tdTomato (Lv-Cont)] or Tfeb [Lv-Tfeb-IRES-tdTomato (Lv-Tfeb)]. Accumulated LC3 was considerably reduced in Lv-Tfeb-transduced compared with that of Lv-Cont-transduced dKO MuSCs without Baf treatment, while

increased upon Baf treatment (*Figure* 3G and 3H), indicating that impaired autophagosome clearance in dKO MuSCs was rescued by Tfeb overexpression. Consistently, the expressions of *p16* and *p21* were significantly reduced in Lv-Tfeb MuSCs compared with those in Lv-Cont MuSCs (*Figure* 3I). To test whether the transduction of Tfeb also restores regenerative dysfunction of dKO MuSCs, we transplanted Lv-Cont-transduced or Lv-Tfeb-transduced dKO MuSCs into MuSC-depleted *Pax7^{CreER}*;*ROSA-DTA* mice that were pre-injured with $BaCl_2$ 1 day before transplantation. After muscle regeneration, all myofibres containing centralized myonuclei could be considered to be originated from donor MuSCs, because recipient mice lack MuSCs.[39] Notably, Lv-Tfeb-transduced dKO MuSCs showed extensive muscle regeneration compared with that of controls (*Figure* 3J–3K).

Inhibition of the hypothalamic–pituitary–gonadal axis provokes muscle stem cells into senescence

Dysfunction of the HPG axis upon menopause/andropause is one of the physiopathological problems resulting in age-related diseases in aging organisms.[14,40–42] To investigate the physiological relevance of our findings that the HPG axis controls autophagosome clearance in MuSCs via Tfeb, we administered Nal-Lys GnRH antagonist (Antide) into young mice to establish a model that interferes with the HPG axis.[43] As expected, serum levels of sex steroid hormones were considerably decreased by Antide treatment, resembling the levels of geriatric mice (*Figure* S4A and *Table* S2). To examine whether the GnRH-sex hormones axis indeed regulates autophagosome clearance in MuSCs *in vivo*, we administered Antide to young GFP-LC3 mice for 4 months. GFP-LC3 puncta were accumulated in MuSCs from Antide-treated GFP-LC3 mice even without Baf treatment (*Figure* 4A–4C), indicating their inability to clear autophagosomes as reported in geriatric MuSCs.[19] As in dKO mice (*Figure* 4E), *Tfeb* and Tfeb target gene expression were reduced in MuSCs from Antide-treated mice compared with those in controls (*Figure* 4D). These data suggest that the HPG-sex hormone axis regulates the autophagy elimination system through Tfeb in MuSC.

To further investigate whether GnRH inhibition leads to the inability of autophagosome clearance causing MuSC senescence, we assessed the autophagy flux and senescence-associated changes in young GFP-LC3 mice treated with Antide for 2 months (*Figure* S4B). Although short-term treatment of Antide resulted in no alteration of senescence markers, it showed an inability of autophagosome clearance compared with those of controls (*Figure* S4C–S4E), which were similar to those of aged (20–24 months) mice.[9] However, long-term treatment of Antide more than 6 months lead to increased γH2AX, SA-β-Gal activity, and senescence-associated genes in MuSCs compared with those of controls, which were similar to those of geriatric MuSCs (*Figure* S5A–
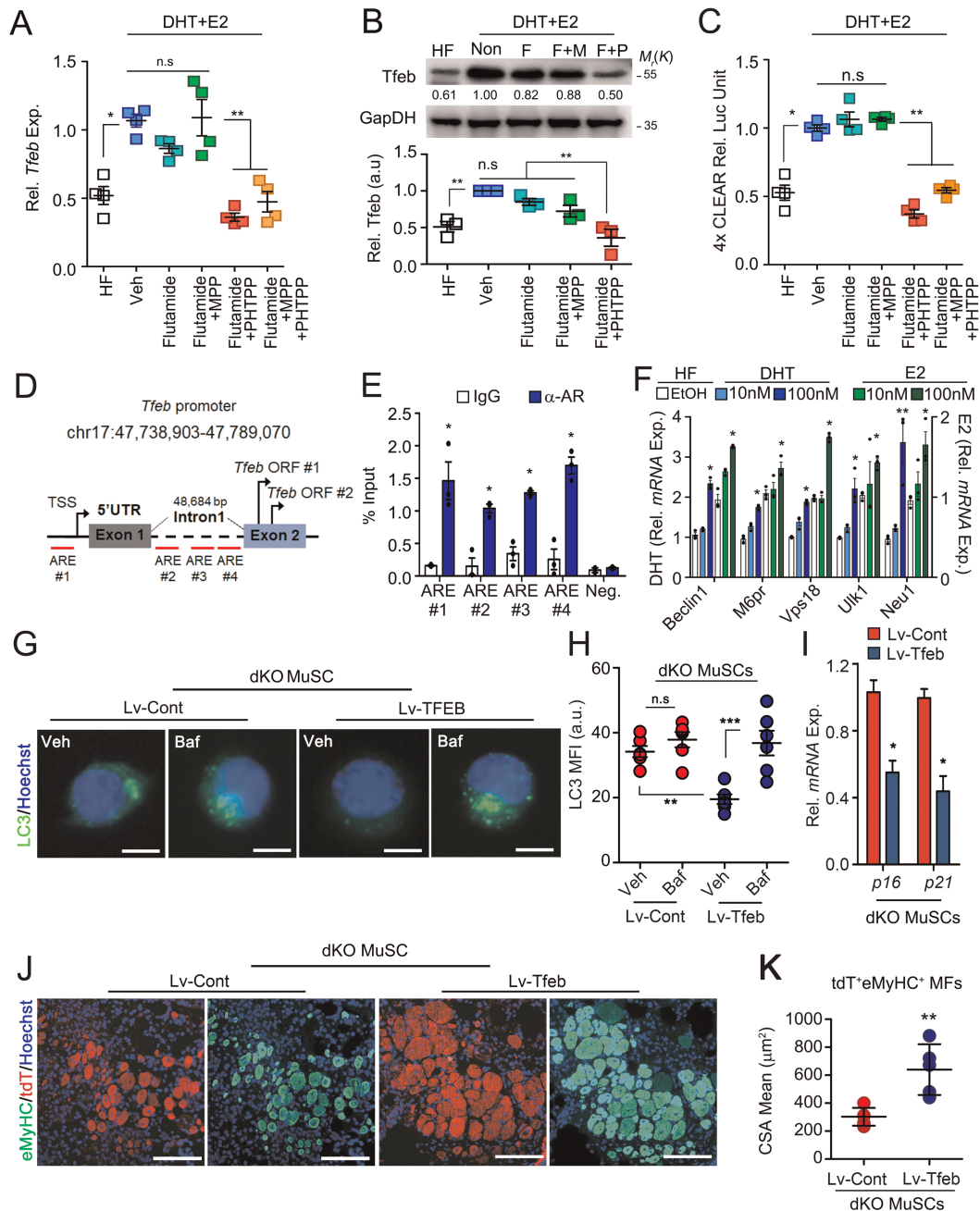
Figure 3 Transcriptional regulation of Tfeb by androgen receptor and oestrogen receptor beta signalling. (A) Relative mRNA expression of Tfeb in C2C12 cells treated with indicated inhibitors for 12 h. HF, hormone-free media; F, Flutamide, an Ar inhibitor; M, MPP, an Esr1 inhibitor; P, PHTPP, an Esr2 inhibitor. (B) Representative immunoblot (top) of Tfeb and relative band densities (bottom) in C2C12 cells treated with the inhibitors for 24 h. (C) Relative luciferase units (RLU) of CLEAR motif sequence in C2C12 cells expressing 4× CLEAR treated with the inhibitors for 24 h. (D) Putative binding sites of Ar in the *Tfeb* gene. TSS, transcription start site; ORF, open reading frame. (E) Chromatin-immunoprecipitation analysis of MuSCs from skeletal muscles of 4-month-old mice with control IgG and anti-Ar antibody. (F) mRNA expressions of Tfeb target-genes in C2C12 cell treated with DHT (right y axis) or 17β-estradiol (left y axis) for 24 h. (G–K) Three-month-old WT and dKO mice were orally administered with tamoxifen for 5 days, and then, MuSCs were isolated from hindlimb muscles 6 months after tamoxifen treatment. MuSCs transduced with lentiviral vectors containing control or Tfeb [Lv-Cont-IRES-tdTomato (Lv-Cont) or Lv-Tfeb-IRES-tdTomato (Lv-Tfeb)]. MuSCs were analysed 96 h after Tfeb transduction. Immunostaining for LC3 (G) and quantification of MFI (H) with or without Baf treatment for 6 h. Relative mRNA expression of senescence-associated genes (I). (J and K) Sixteen hours after transduction, equal numbers of transduced MuSCs were transplanted into young injured *Pax7^CreER^;ROSA-DTA* mice pre-treated with tamoxifen for 4 weeks before injury. Ten days after MuSC transplantation, TA muscles were analysed. IHC images for eMyHC and tdTomato (J), and quantification of mean CSA of tdT⁺eMyHC⁺ myofibres (K). Comparisons by one-way ANOVA with Tukey's post hoc test (A–C, F, and H) and unpaired *t*-test (E). Scales: 10 (G) and 100 μm (J) bars, mean ± SEM; n = 3–4 independent experiments; *$P < 0.05$, **$P < 0.01$, n.s. not significant. dKO, double knockout; MuSCs, muscle stem cells.
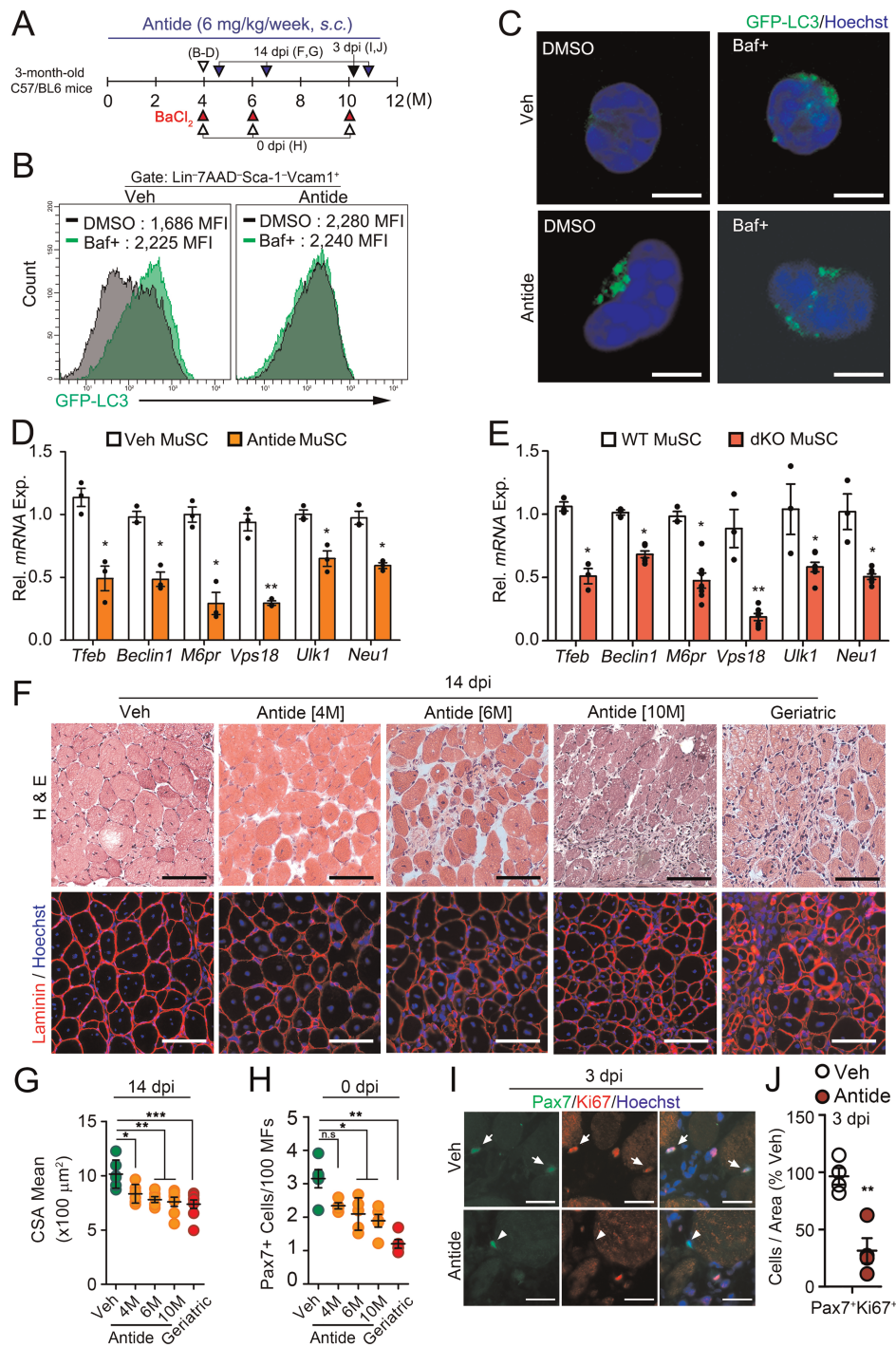
Figure 4 Impaired autophagosome clearance and regenerative function of MuSCs under reduction of HPG-sex steroid hormone-Tfeb axis. (A) A scheme for Antide treatment. Three-month-old mice were subcutaneously injected with vehicle (Veh) or Nal-Lys GnRH antagonist (Antide) for 4, 6, or 10 months. (B and C) MuSCs were isolated from Veh or Antide-treated GFP-LC3 transgenic mice for 4 months and treated with DMSO or Baf for 6 h. Flow cytometry (B) and representative confocal images (C) for GFP-LC3 in MuSCs. (D and E) *Tfeb* and Tfeb target-gene expressions in MuSCs isolated from Antide-treated mice in *Figure*4B (D) and dKO mice in *Figure*1A (E). (F) TA muscles of Antide-treated mice for indicated time were injured by BaCl2 injection and were analysed at 14 dpi. Haematoxylin and eosin (H&E) staining (top) and IHC staining for laminin (bottom). Geriatric mice were 30 months old. (G) Quantifications of CSA of regenerating MFs. (H) The number of Pax7 + cells per 100 MFs in uninjured Veh, Antide-treated, and geriatric TA muscles. (I and J) TA muscles from Antide-treated mice for 10 months were injured by BaCl$_2$ and analysed at 3 dpi. Representative images for Pax7 and Ki67 staining (I) and quantifications (J). Arrows and arrowheads indicate Pax7 $^+$Ki67 $^+$ and Pax7 $^+$Ki67 $^-$ cells, respectively. Scales, 5 (C), 50 (I), and 100 μm (E). Comparisons by one-way ANOVA with Tukey's post hoc test (G–H), Mann–Whitney U test (J) and unpaired *t*-test (D–E). Bars, mean ± SEM; *n* = 4–5 animals per group; *P < 0.05, **P < 0.01. dKO, double knockout; MuSCs, muscle stem cells; WT, wild-type.

S5E). The *ex vivo* colony-forming ability of Antide-treated MuSCs was comparable with that of geriatric MuSCs (*Figure* S5F–S5G and *Movie* S1–S3). Consistently, Antide administration results in numerical and functional decline of MuSCs and defective muscle regeneration (*Figure* 4F–4J). Thus, impaired autophagosome clearance by ablation of the HPG axis accelerates the age-associated defects of MuSCs.

Antide-induced senescence does not associate the Notch signalling pathway

We previously reported that the HPG axis at puberty activates Notch signalling in MuSCs by inducing *Mib1* expression in myofibres at puberty.[16] Thus, the advanced senescence of MuSCs by GnRH inhibition could be due to defective Notch signalling in MuSCs. Therefore, we examined the expression of Notch target genes, *Hes1*, *Hey1*, and *HeyL*, in MuSCs and *Mib1* in myofibres, respectively. Notch-related gene expressions in Antide-treated MuSCs and myofibres were comparable with those of Veh-treated controls (*Figure* S6A and S6B), suggesting that Antide treatment did not completely block, but reduce sex hormone secretion, which is insufficient to inhibit Notch signalling in adult MuSCs.

To further address whether the advanced senescence of MuSCs in Antide-treated mice is not due to defective Notch signalling, we specifically activated Notch signalling in adult MuSCs with Tamoxifen in *Pax7*[CreER]*;ROSA-N1ICD* reporter mice (N1[SC/OE])[44,45] and then administered Antide for 10 months (*Figure* 5A). Because *ROSA-N1ICD* reporter mice coexpress N1ICD with GFP after Cre recombination, we compared GFP[+] and GFP[−] MuSCs to examine whether Notch signalling is implicated in cellular senescence. Expression levels of Notch target genes *Hes1*, *Hey1*, and *HeyL* were considerably increased in GFP[+] MuSCs compared with levels in GFP[−] MuSCs (*Figure* 5B and 5C). Interestingly, however, regardless of Notch activation, both GFP[+] and GFP[−] MuSCs showed similar levels of senescence markers (*Figure* 5C), γH2AX, and DNA damage (*Figure* 5D–5F). These data show that the enhanced senescence by GnRH inhibition is independent of Notch signalling and is more susceptible to low levels of sex steroid hormones.

Sex hormone replacement prevents Antide-induced senescence and muscle stem cell dysfunction

To investigate that MuSC senescence by disrupting the HPG axis is prevented by restoring sex steroid hormones, we performed DHT replacement experiment in Antide-treated mice and examined senescent phenotypes in MuSCs (*Figure* 5G). The senescent phenotypes and dysfunction of the MuSCs were prevented in Antide-treated mice by coadministration of DHT (*Figure* 5H–5L), suggesting that the HPG-sex hormone axis prevents the senescence of MuSCs in adulthood.

Because *Tfeb* expression was decreased in geriatric MuSCs compared with that of young MuSCs (*Figure* S7A), we examined whether decreased Tfeb expression is responsible for impaired autophagosome clearance and senescence in geriatric MuSCs. Interestingly, LC3 accumulation significantly reduced by Lv-Tfeb transduction compared with Lv-Cont transduction in geriatric MuSCs without Baf treatment, while increased by Bafilomycin treatment (*Figures* 6A, 6B, and S7B), indicating that impaired autophagy flux in the geriatric MuSCs was rescued by Tfeb expression. Consistently, the expressions of autophagy/lysosomal genes and senescence markers, *p16* and *p21*, were significantly restored in Lv-Tfeb-transduced geriatric MuSCs compared with those in Lv-Cont-transduced geriatric MuSCs (*Figures* 6C and S7C). Moreover, the percentage of EdU[+] MuSCs and colonies of cultured MuSCs were significantly increased in Lv-Tfeb-transduced geriatric MuSCs compared with those of controls (*Figures* 6D, 6E, and S7D–F).

Finally, to examine whether the transduction of Tfeb in geriatric MuSCs can rescue the impaired regenerative function of MuSCs, we transduced Tfeb-IRES-tdTomato-expressing lentivirus into geriatric MuSCs and transplanted them into MuSC-depleted *Pax7*[CreER]*;ROSA-DTA* mice, in which transplanted donor MuSCs are a major contributor to muscle mass and myofibre formation (*Figure* 6F). Consistent with our findings above, the transduction of the Tfeb in naturally aged MuSCs greatly increased myogenic functions (*Figure* 6G–6J). Taken together, our data show that sex steroid hormones governed by the HPG axis systemically control autophagosome clearance in MuSCs through Tfeb and prevent MuSCs from senescence.

Discussion

Serum levels of testosterone and estradiol, which gradually increase after pubertal onset, are maintained by the HPG axis throughout adulthood, and finally decrease in old age.[16,17,47] We previously reported that increased sex hormones by the HPG axis at puberty establish a reservoir of adult MuSCs.[16] We show here that increased and sustained levels of sex hormones at adulthood prevent MuSC senescence by maintaining autophagosome clearance through Tfeb, and their decline at old age results in the reduction of Tfeb that leads to accumulation of autophagosome and eventual induction of senescence at geriatric age (*Figure* 7). Our data suggest that the HPG-sex hormone axis is one of the master regulators of MuSCs throughout life.

As organism ages, MuSCs become defective in autophagy flux leading to the accumulation of autophagosome.[9] Using Atg7-ablated MuSCs, Garcia-Prat *et al.* reported that autophagy impairment-induced p16 expression provokes entry into senescence and impairs MuSC functions, suggesting that autophagy prevents MuSCs from senescence. However,
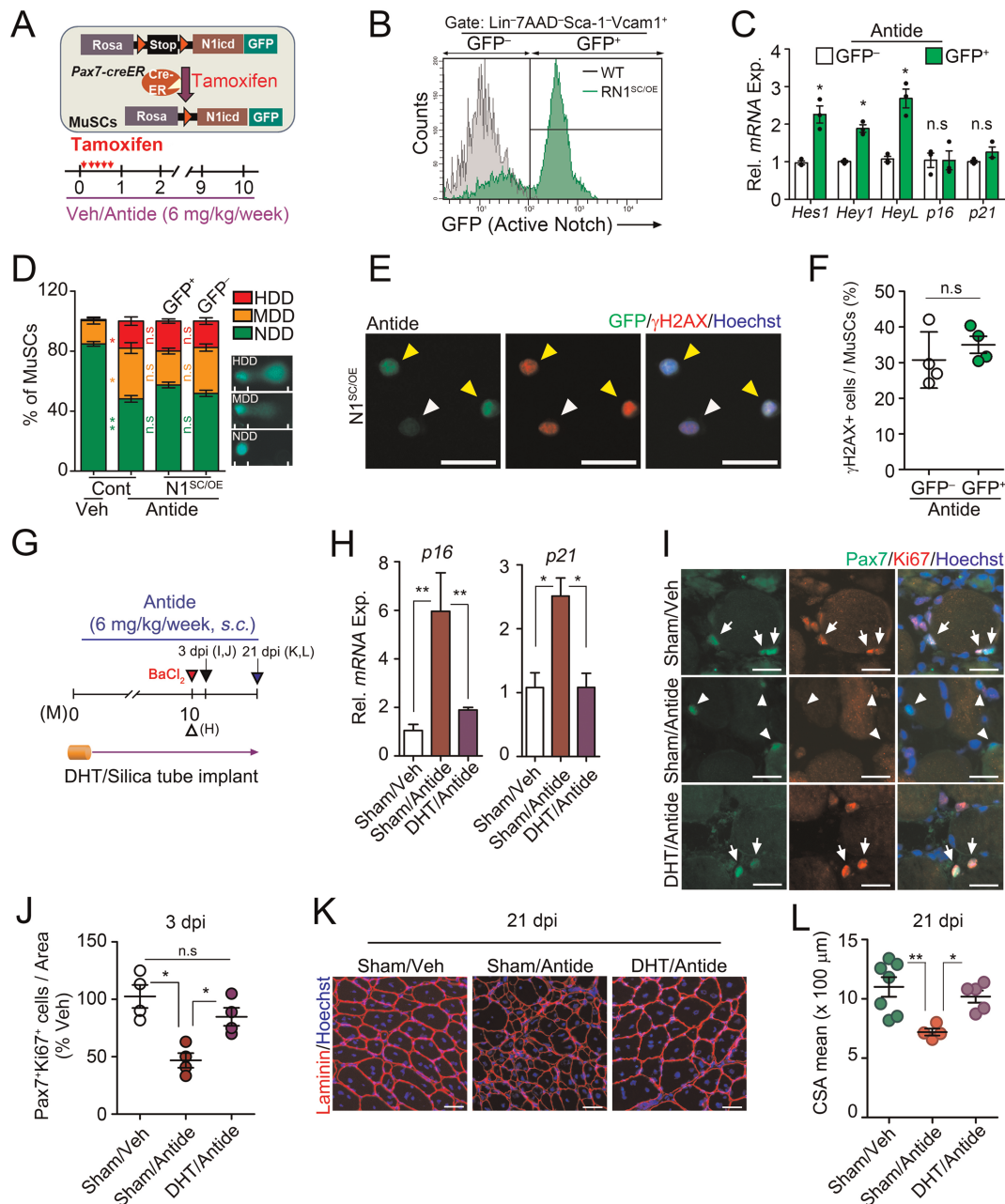
Figure 5 Prevention of Antide-induced muscle stem cell (MuSC) senescence by sex hormone administration, not by Notch signalling activation. (A–F) Three-month-old WT and *Pax7^{CreER};ROSA-N1* (N1$^{SC/OE}$) transgenic mice were orally administered with Tmx for five consecutive days and treated with Antide for 10 months as indicated. Note that GFP in MuSCs from *Pax7^{CreER};ROSA-N1* (N1$^{SC/OE}$) mice is coexpressed with the intracellular domain of Notch1 after successful recombination by Cre recombinase. A scheme for MuSC-specific activation of Notch signalling (top) and Antide administration (bottom) (A). Flow cytometry analysis of MuSCs isolated from Antide-treated WT or N1$^{SC/OE}$ mice. Note that GFP$^+$ and GFP$^-$ cells are N1ICD-overexpressing and normal MuSCs, respectively, in one mouse (B). Relative mRNA expression of Notch target genes and senescence-associated genes in GFP$^+$ and GFP$^-$ MuSCs isolated from Antide-treated N1$^{SC/OE}$ mice (C). Quantification of single-cell electrophoretic assay (D). Veh-treated or Antide-treated WT mice were used as control group (Cont). Note that a distinct head and tail by single cell electroporation mean intact DNA and bro-ken pieces of damaged DNA, respectively.[46] Representative images for γH2AX and GFP in freshly isolated MuSCs (E) and quantification (F). (G–L) A scheme for Antide and DHT cotreatment. Silastic tubes containing Veh or DHT were implanted into 3-month-old C57BL/6 mice, and they were treated with Antide 6 mg/kg/week for 10 months (G). Relative mRNA expression of senescence-associated genes in MuSCs from Sham/Veh, Sham/Antide or DHT/Antide-treated mice (H). BaCl$_2$ injury was induced in TA muscles of indicated mice. At 3 dpi, representative images (I) and relative percentages of Pax7$^+$Ki67$^+$ cells (J). Arrows and arrowheads indicate Pax7$^+$Ki67$^+$ and Pax7$^+$Ki67$^-$ cells, respectively. IHC images for laminin (K) and (L) quantification of CSA of TA muscles at 21 dpi. Scales: 100 (H) and 50 μm (E). Comparisons by one-way analysis of variance with Tukey's post hoc test and paired *t*-test. Bars, mean ± SEM; 4 animals per group and K; *n* = 7 (Sham/Veh), 4 (Sham/Antide), and 5 (DHT/Antide) TA muscles from 4 animals per group; *$P < 0.05$, **$P < 0.01$, n.s. not significant.
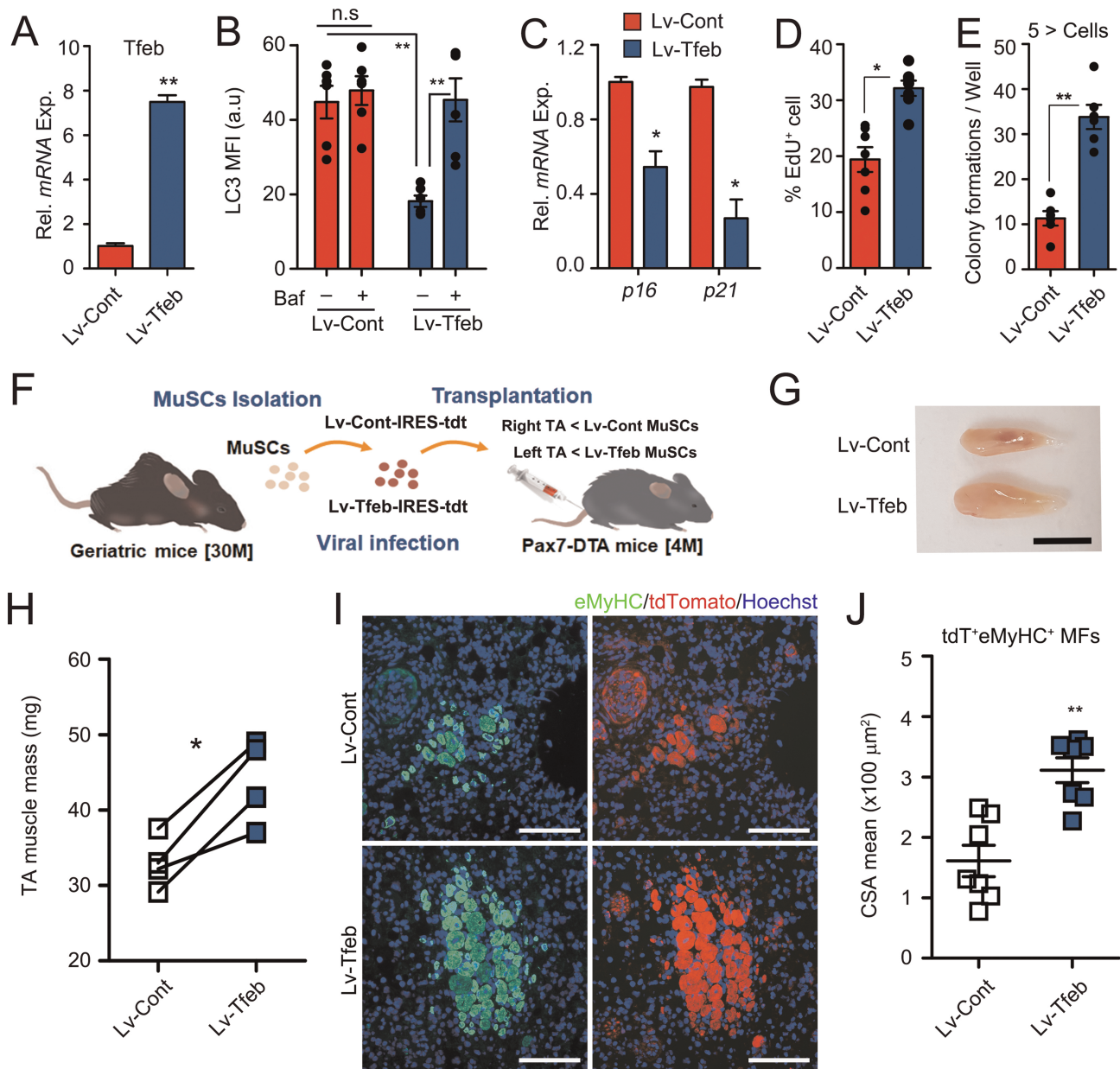
Figure 6 Improved function of geriatric muscle stem cells (MuSCs) by Tfeb overexpression. (A–E) Geriatric MuSCs were transduced with Lv-Cont and Lv-Tfeb lentivirus. Seventy-two hours after transduction, Tfeb expression (A) and quantification of MFI for LC3 proteins with or without Baf for 6 h (B). Relative expressions of p16 and p21 in transduced MuSCs (C). Percentages of EdU + cells (D) and number of colony formation (E) 96 h after transduction. Representative images for EdU incorporation and colony formation assays of the MuSCs were shown in *Figure*S7D and S7E. Cell clusters consisting of at least five or more cells were counted as colony. (F) A scheme for MuSC transplantation. Equal numbers of 16 h of transduced geriatric MuSCs were transplanted into young injured Pax7[CreER];ROSA-DTA mice pre-treated with tamoxifen for 4 weeks before injury. Ten days after MuSC transplantation, the TA muscles were analysed. (G) Gross morphology and (H) muscle mass of TA muscles. (I) IHC images for eMyHC and tdTomato, and (J) quantification of mean CSA for tdT + eMyHC + myofibres. Scales: 0.5 cm (G) and 100 μm (I). Comparisons by Mann–Whitney U test (B, D, E, and H) and unpaired *t*-test (A, C, and J). Bars, mean ± SEM; *n* = 4–7 animals per group; *P < 0.05, **P < 0.01, n.s. not significant.

autophagosome formation itself was impaired in the Atg7-ablated MuSCs,[9,13] detailed mechanism by which autophagy prevents senescence of naturally aged MuSCs remained to be elucidated. In this study, genetic and pharmacological inhibition of the HPG axis recapitulates progressive aging progress of MuSCs: at early stage, decrease of Tfeb,

autophagy, and lysosomal genes leads to impaired autophagosome clearance, which is similar to those of old MuSCs.[9] At late stage, however, a gradual increase of ROS by prolonged inhibition of the HPG axis reaches the level similar to that of geriatric MuSCs and eventually provokes entry into senescence (*Figure* 7). Thus, circulating sex hormonal
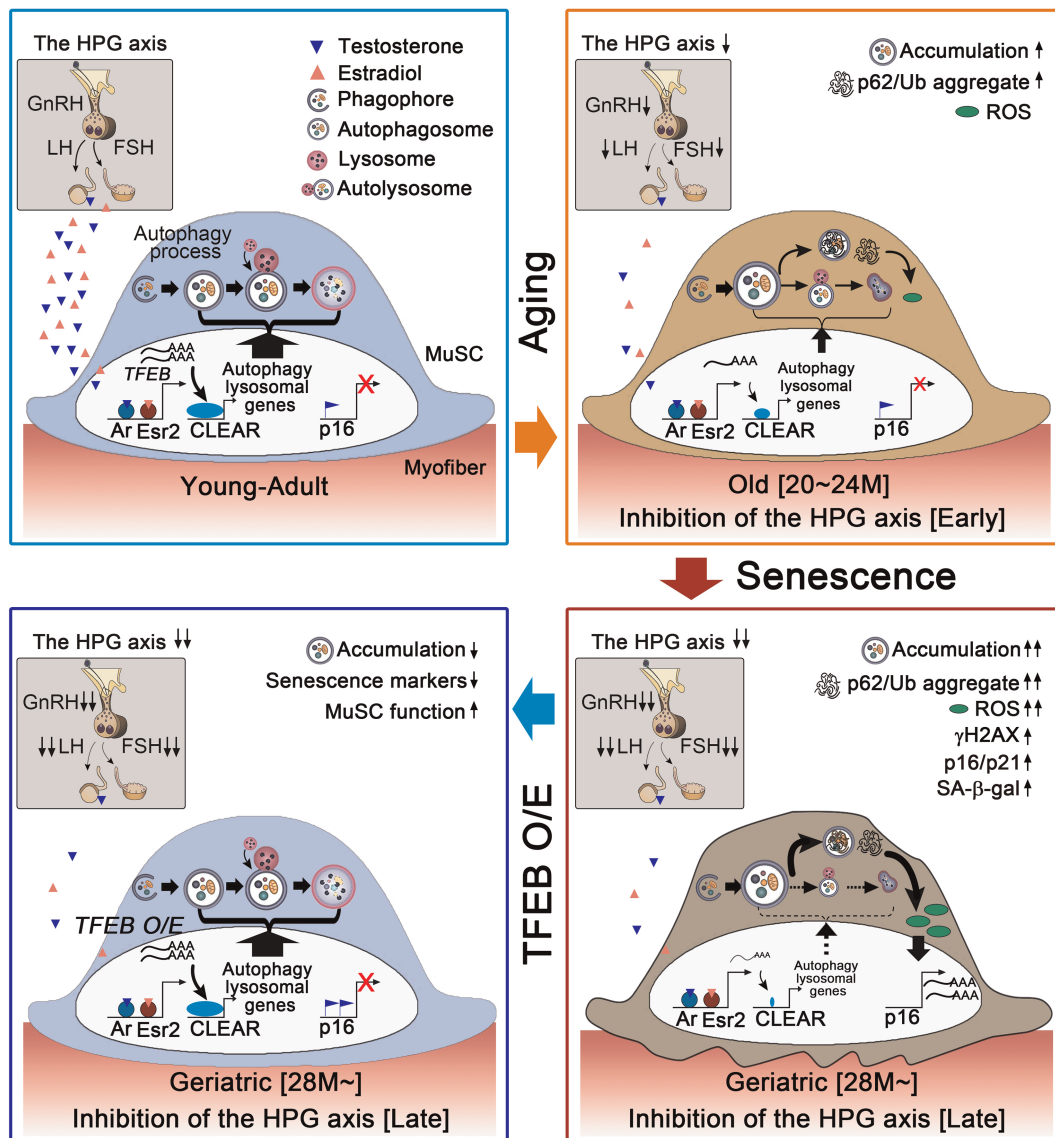
Figure 7 A proposed model. In youthful environment, sex steroid hormones controlled by the HPG axis transcriptionally induce the expression of Tfeb in muscle stem cells (MuSCs). Tfeb drives the expression of the entire network of genes that contain the coordinated lysosomal expression and regulation (CLEAR) motif in their promoters. Accordingly, the autophagy–lysosome pathway maintains stemness and quiescence of MuSCs. However, at early stage, decreased sex hormone signalling by functional decline of the HPG axis at old age or inhibition of GnRH results in decrease of Tfeb and autophagy and lysosomal genes, which leads to impaired autophagosome clearance and accumulation of bulk autophagy substrates (LC3, p62/Ub) and ROS. At late stage, the gradual increase of ROS by prolonged decrease of the HPG axis reaches the level similar to that of geriatric MuSCs and then eventually provokes entry into senescence, which is relevant to an organism's normal aging process: impaired autophagy clearance at an early stage and then cellular senescence at the late stage. Importantly, Tfeb overexpression in geriatric or sex hormone signalling-disrupted MuSCs rescues impaired autophagy–lysosome system and reverts MuSC function. Therefore, the HPG-Tfeb axis would be a key contributor to the aging of MuSCs. HPG, hypothalamic–pituitary–gonadal.

diminution is causally implicated in the physiological progress of MuSC aging and senescence. In accordance with the hypothalamic control of systemic aging,[14,15] our study showed that decreased levels of GnRH result in the reduction of sex hormone secretion, Tfeb expression, and autophagosome clearance. Recently, Leeman *et al.*[31] reported that constitutive activation of Tfeb in old quiescent neural stem cells allows them to regain a more youthful state.

Therefore, the HPG-sex hormone-Tfeb axis will prevent the aging of quiescent adult stem cells such as MuSCs and neural stem cells possibly by inducing autophagosome clearance.

In this study, the HPG-sex hormone axis directly regulates the autophagy and lysosome pathway through the transcriptional induction of Tfeb in a MuSC-intrinsic manner. In parallel, the same axis induces Mib1 in myofibres to activate Notch signalling in MuSCs at puberty, as reported.[16] Each pathway

leads to different outcomes, although both are crucial for adult MuSC homeostasis. The former maintains MuSC quiescence, while the latter establishes adult quiescent MuSCs and prevents premature differentiation of MuSCs. Notch inhibition results in myogenic differentiation of MuSCs without entering the S phase that leads to depletion of MuSCs, while Notch activation confers stemness to MuSCs by preventing their differentiation.[44,48,49] In fact, myofibre-specific disruption of Mib1 leads to the depletion of MuSCs in adult mice, in which the sex hormone–autophagy–lysosome system remains intact (manuscript in preparation). By contrast, in both Antide-treated *Pax7^{CreER};ROSA-N1ICD* transgenic mice and dKO mice, in which Notch signalling is constitutively active and intact, respectively, MuSCs show an intrinsic functional impairment that is representative of premature aging. These data indicate that the sex hormone–autophagy–lysosome system is also critical for the maintenance of quiescent MuSCs by preventing enhanced senescence. In conclusion, the HPG-sex hormone axis plays dual roles by activating the autophagy–lysosome system to maintain quiescent MuSCs and by activating Notch signalling to prevent premature differentiation of MuSCs throughout life.

Funding

Author contributions

J.H.K. designed the study, performed the experiments, and wrote the manuscript. I.P., H.S., J.R., J.Y.S., J.P., K.Y., S.H.H., J.S.K., Y.W.J., and Y.L.K. conducted the experiments. J.Y.M. and M.H.C. performed serum steroid profiling using GC-MS/MS. Y.Y.K. designed the research and wrote the manuscript.

Acknowledgements

Online supplementary material

Additional supporting information may be found online in the Supporting Information section at the end of the article.

Data S1 Supporting Information

Movie S1 Supporting Information

Movie S2 Supporting Information

Movie S3 Supporting Information

Table S1. List of autophagy-related and lysosomal genes

Table S2. Representative mass-spectrometric chromatogram and result of steroid profiling for blood samples.

Data S2. The hypothalamic-pituitary-gonadal axis controls muscle stem cell senescence through autophagosome clearance

Conflict of interest

The authors declare no competing financial interests. Correspondence and requests for materials should be addressed to Y.Y.K. (ykong@snu.ac.kr).

Ethical statement

All authors in this manuscript certify the ethical guidelines for authorship and publishing in the Journal of Cachexia, Sarcopenia and Muscle.[50]

References

1. Lepper C, Partridge TA, Fan CM. An absolute requirement for Pax7-positive satellite cells in acute injury-induced skeletal muscle regeneration. *Development* 2011;**138**:3639–3646.

2. Relaix F, Zammit PS. Satellite cells are essential for skeletal muscle regeneration: the cell on the edge returns centre stage. *Development* 2012;**139**: 2845–2856.

3. Conboy IM, Conboy M, Wagers A, Girma E, Weissman I, Rando TA, et al. Rejuvenation of aged progenitor cells by exposure to a young systemic environment. *Nature* 2005;**433**:760–764.

4. Chakkalakal JV, Jones KM, Basson MA, Brack AS. The aged niche disrupts muscle stem cell quiescence. *Nature* 2012;**490**:355–360.

5. Schwörer S, Becker F, Feller C, Baig AH, Köber U, Henze H, et al. Epigenetic stress responses induce muscle stem-cell ageing by Hoxa9 developmental signals. *Nature* 2016;**540**:428–432.

6. Sousa-Victor P, Perdiguero E, Muñoz-Ćanoves P. Geroconversion of aged muscle stem cells under regenerative pressure. *Cell Cycle* 2014;**13**:3183–3190.

7. Brack AS, Muñoz-Cánoves P. The ins and outs of muscle stem cell aging. *Skeletal muscle* **6**:1–9.

8. Baghdadi MB, Castel D, Machado L, Fukada SI, Birk DE, Relaix F, et al. Reciprocal signalling by Notch-Collagen V-CALCR retains muscle stem cells in their niche. *Nature* 2018;**557**:714–718.

9. García-Prat L, Martínez-Vicente M, Perdiguero E, Ortet L, Rodríguez-Ubreva J, Rebollo E, et al. Autophagy maintains stemness by preventing senescence. *Nature* 2016;**529**:37–42.

10. Steffen KK, Dillin A. A ribosomal perspective on proteostasis and aging. *Cell Metab* 2016;**23**:1004–1012.

11. García-Prat L, Sousa-Victor P, Muñoz-Cánoves P. Proteostatic and metabolic control of stemness. *Cell Stem Cell* 2017;**20**:593–608.

12. Mizushima N. Autophagy: process and function. *Genes Dev* 2007;**21**:2861–2873.

13. Zhang Y, Goldman S, Baerga R, Zhao Y, Komatsu M, Jin S. Adipose-specific deletion of autophagy-related gene 7 (atg7) in mice reveals a role in adipogenesis. *Proc Natl Acad Sci U S A* 2009;**106**:19860–19865.

14. Zhang G, Li J, Purkayastha S, Tang Y, Zhang H, Yin Y, et al. Hypothalamic programming of systemic ageing involving IKK-β, NF-κB and GnRH. *Nature* 2013;**497**:211–216.

15. Zhang Y, Kim MS, Jia B, Yan J, Zuniga-Hertz JP, Han C, et al. Hypothalamic stem cells control ageing speed partly through exosomal miRNAs. *Nature* 2017;**548**:52–57.

16. Kim JH, Han GC, Seo JY, Park I, Park W, Jeong HW, et al. Sex hormones establish a reserve pool of adult muscle stem cells. *Nat Cell Biol* 2016;**1**:930–940.

17. Seo JY, Kim JH, Kong YY. Unraveling the paradoxical action of androgens on muscle stem cells. *Mol Cells* 2019;**42**:97–103.

18. Shiina H, Matsumoto T, Sato T, Igarashi K, Miyamoto J, Takemasa S, et al. Premature ovarian failure in androgen receptor-deficient mice. *Proc Natl Acad Sci U S A* 2006;**103**:224–229.

19. Mizushima N, Yamamoto A, Matsui M, Yoshimori T, Ohsumi Y. In vivo analysis of autophagy in response to nutrient starvation using transgenic mice expressing a fluorescent autophagosome marker. *Mol Biol Cell* 2004;**15**:1101–1111.

20. Liu L, Cheung TH, Charville GW, Hurgo BMC, Leavitt T, Shih J, et al. Chromatin modifications as determinants of muscle stem cell quiescence and chronological aging. *Cell Rep* 2013;**4**:189–204.

21. Kitajima Y, Ono Y. Estrogens maintain skeletal muscle and satellite cell functions. *J Endocrinol* 2016;**229**:267–275.

22. Velders M, Schleipen B, Fritzemeier KH, Zierau O, Diel P. Selective estrogen receptor-beta activation stimulates skeletal muscle growth and regeneration. *FASEB J* 2012;**26**:1909–1920.

23. Sinha-Hikim I, Taylor WE, Gonzalez-Cadavid NF, Zheng W, Bhasin S. Androgen receptor in human skeletal muscle and cultured muscle satellite cells: up-regulation by androgen treatment. *J Clin Endocrinol Metab* 2004;**89**:5245–5255.

24. van Deursen JM. The role of senescent cells in ageing. *Nature* 2014;**509**:439–446.

25. Bae JH, Hong M, Jeong HJ, Kim H, Lee SJ, Ryu D, et al. Satellite cell-specific ablation of Cdon impairs integrin activation, FGF signalling, and muscle regeneration. *J Cachexia Sarcopenia Muscle* 2020;**11**:1089–1103.

26. Chang BD, Watanabe K, Broude EV, Fang J, Poole JC, Kalinichenko TV, et al. Effects of p21Waf1/Cip1/Sdi1 on cellular gene expression: implications for carcinogenesis, senescence, and age-related diseases. *Proc Natl Acad Sci U S A* 2000;**97**:4291–4296.

27. Baker DJ, Childs BG, Durik M, Wijers ME, Sieben CJ, Zhong J, et al. Naturally occurring p16(Ink4a)-positive cells shorten healthy lifespan. *Nature* 2016;**530**:184–189.

28. Shin HJR, Kim H, Oh S, Lee JG, Kee M, Ko HJ, et al. AMPK–SKP2–CARM1 signalling cascade in transcriptional regulation of autophagy. *Nature* 2016;**534**:553–557.

29. Settembre C, Di Malta C, Polito VA, Arencibia MG, Vetrini F, Erdin S, et al. TFEB links autophagy to lysosomal biogenesis. *Science* 2011;**332**:1429–1433.

30. Manchon JFM, Uzor NE, Kesler SR, Wefel JS, Townley DM, Nagaraja AS, et al. TFEB ameliorates the impairment of the autophagy-lysosome pathway in neurons induced by doxorubicin. *Aging (Albany NY)* 2016;**8**:3507–3519.

31. Leeman DS, Hebestreit K, Ruetz T, Webb AE, McKay A, Pollina EA, et al. Lysosome activation clears aggregates and enhances quiescent neural stem cell activation during aging. *Science* 2018;**359**:1277–1283.

32. Carmona-Gutierrez D, Hughes AL, Madeo F, Ruckenstuhl C. The crucial impact of lysosomes in aging and longevity. *Ageing Res Rev* 2016;**32**:2–12.

33. Settembre C, Fraldi A, Medina DL, Ballabio A. Signals from the lysosome: a control centre for cellular clearance and energy metabolism. *Nat Rev Mol Cell Biol* 2013;**14**:283–296.

34. Kaushik S, Cuervo AM. Proteostasis and aging. *Nat Med* 2015;**21**:1406–1415.

35. Farla P, Hersmus R, Trapman J, Houtsmuller AB. Antiandrogens prevent stable DNA-binding of the androgen receptor. *J Cell Sci* 2005;**118**:4187–4198.

36. Sun J, Huang YR, Harrington WR, Sheng S, Katzenellenbogen JA, Katzenellenbogen BS. Antagonists selective for estrogen receptor alpha. *Endocrinology* 2002;**143**:941–947.

37. Hsu I, Chuang KL, Slavin S, Da J, Lim WX, Pang ST, et al. Suppression of ERbeta signaling via ERbeta knockout or antagonist protects against bladder cancer development. *Carcinogenesis* 2014;**35**:651–661.

38. Sardiello M, Palmieri M, di Ronza A, Medina DL, Valenza M, Gennarino VA, et al. A gene network regulating lysosomal biogenesis and function. *Science* 2009;**325**:473–477.

39. Murphy MM, Lawson JA, Mathew SJ, Hutcheson DA, Kardon G. Satellite cells, connective tissue fibroblasts and their interactions are crucial for muscle regeneration. *Development* 2011;**138**:3625–3637.

40. Atwood CS, Meethal SV, Liu T, Wilson AC, Gallego M, Smith MA, et al. Dysregulation of the hypothalamic-pituitary-gonadal axis with menopause and andropause promotes neurodegenerative senescence. *J Neuropathol Exp Neurol* 2005;**64**:93–103.

41. Sipilä S, Törmäkangas T, Sillanpää E, Aukee P, Kujala UM, Kovanen V, et al. Muscle and bone mass in middle-aged women: role of menopausal status and physical activity. *J Cachexia Sarcopenia Muscle* 2020;**11**:698–709.

42. Burney BO, Garcia JM. Hypogonadism in male cancer patients. *J Cachexia Sarcopenia Muscle* 2012;149–155.

43. Gordon K, Williams RF, Danforth DR, Hodgen GD. Antide-induced suppression of pituitary gonadotropin and ovarian steroid secretion in cynomolgus monkeys: premature luteolysis and prolonged inhibition of folliculogenesis following single treatment. *Biol Reprod* 1991;**44**:701–706.

44. Wen Y, Bi P, Liu W, Asakura A, Keller C, Kuang S. Constitutive Notch activation upregulates Pax7 and promotes the self-renewal of skeletal muscle satellite cells. *Mol Cell Biol* 2012;**32**:2300–2311.

45. Murtaugh LC, Stanger BZ, Kwan KM, Melton DA. Notch signaling controls multiple steps of pancreatic differentiation. *Proc Natl Acad Sci U S A* 2003;**100**:14920–14925.

46. Olive PL, Banath JP. The comet assay: a method to measure DNA damage in individual cells. *Nat Protoc* 2006;23–29.

47. Ober C, Loisel DA, Gilad Y. Sex-specific genetic architecture of human disease. *Nat Rev Genet* 2008;**9**:911–922.

48. Mourikis P, Sambasivan R, Castel D, Rocheteau P, Bizzarro V, Tajbakhsh S. A critical requirement for notch signaling in maintenance of the quiescent skeletal muscle stem cell state. *Stem Cells* 2012;**30**:243–252.

49. Bjornson CR, Cheung TH, Liu L, Tripathi PV, Steeper KM, Rando TA. Notch signaling is necessary to maintain quiescence in adult muscle stem cells. *Stem Cells* 2012;**30**:232–242.

50. von Haehling S, Morley JE, Coats AJ, Anker SD. Ethical guidelines for publishing in the Journal of Cachexia, Sarcopenia and Muscle: update 2019. *J Cachexia Sarcopenia Muscle* 2019;**10**:1143–1145.